Transportation Research Part D 89 (2020) 102629

Contents lists available at ScienceDirect

Transportation Research Part D

journal homepage: www.elsevier.com/locate/trd

Quantifying and analyzing traffic emission reductions from ridesharing: A case study of Shanghai

Longxu Yan [a], Xiao Luo [b,*], Rui Zhu [c], Paolo Santi [d,e], Huizi Wang [b], De Wang [a], Shangwu Zhang [a], Carlo Ratti [d]

[a] College of Architecture and Urban Planning, Tongji University, China
[b] College of Transportation Engineering, Tongji University, China
[c] Senseable City Laboratory, Future Urban Mobility IRG, Singapore-MIT Alliance for Research and Technology, Singapore
[d] Senseable City Laboratory, Department of Urban Studies and Planning, Massachusetts Institute of Technology, USA
[e] Istituto di Informatica e Telematica del CNR, Pisa, ITALY

ARTICLE INFO

Keywords:
Ridesharing
Traffic emission
Shareability network
Spatiotemporal patterns

ABSTRACT

Ridesharing has potential to mitigate traffic emissions. To better support policymaking, this paper endeavors to estimate and analyze emission reductions by large-scale ridesharing combining the Shareability-Network approach, the COPERT III emission model, and a speed-density traffic-flow model. Using Shanghai as a case, we show that ridesharing *per se* can reduce fuel-consumption (FC) by 22.88% and 15.09% in optimal and realistic scenarios, respectively, with corresponding emissions reductions. Ridesharing's spontaneous first-order speed effect further reduces FC by 0.34–0.96%. Additionally, spatial analyses show that ridesharing reduces more emissions on severely polluted roads, leading to two spatial patterns; temporal analyses demonstrate patterns shifted from disorganized to organized. Both the phenomena can be explained by the aggregation of trips and the grading and topology of the roads. Moreover, ridesharing may also increase emissions on some branch roads, creating a new environmental injustice, which, however, is estimated to be less significant than expected.

1. Introduction

Traffic emissions in China have become one of the primary sources of urban pollution, causing significant environmental degradation and health hazard (Xue et al., 2010). According to the *China Vehicle Environmental Management Annual Report* (China Vehicle Environmental Management Annual Report, 2018), traffic emission has become the primary source of $PM_{2.5}$ in Beijing, Shanghai, Hangzhou, Guangzhou, Shenzhen, and Jinan and the secondary source in many other big cities including Nanjing, Wuhan, etc. Automobiles have contributed more than 80% of the total carbonic oxide (CO) and hydrocarbon (HC) emissions and more than 90% of the total oxy-nitride (NOx) or particulate matter (PM) production. How to mitigate traffic emissions without hurting access to convenient mobility options, travelers' feeling, and the economic growth, has become a realistic and urgent problem faced by urban researchers and planners, transportation policymakers, enterprises, and the public around the world (Gorham, 2002).

Shared mobility, possibly combined with autonomous driving and electrification, are widely recognized as having the potential to decrease traffic emission (Brown et al., 2014; Litman, 2013). Emerging shared mobility models can be summarized into mainly three

* Corresponding author at: College of Transportation Engineering, Tongji University, 1239 Siping Road, Shanghai 200092, China.
E-mail address: luo.xiao@tongji.edu.cn (X. Luo).

https://doi.org/10.1016/j.trd.2020.102629

Available online 17 November 2020

categories (Jin et al., 2018; Shaheen et al., 2016): (1) Vehicle sharing (Hu, Chen, et al., 2018; Hu et al., 2019; Hu, Lin, et al., 2018). However, as long as self-driving technology has not been fully operated yet, vehicle sharing remains incapable of providing on-demand, point-to-point ride services. (2) Ridesourcing, which refers to transportation services connecting community drivers with passengers via mobile applications. Although ridesourcing has been expanding rapidly across the world with a number of successful TNCs (Transport-Network-Companies), such as Uber and Lyft in the U.S., Didi in China, and Ola in India, its environmental impact is still uncertain (Jin et al., 2018). And, (3) ridesharing, that allows multiple passengers with similar origins and destinations to share a ride. Unlike categories (1) and (2), ridesharing is not only practical to provide on-demand services but has been proved effective in reducing VMT (Vehicle-Miles-Traveled), hence traffic emissions, in simulation-based studies (Santi et al., 2014a; Yin et al., 2018).

However, current literature mainly focuses on evaluating the *overall* benefits of ridesharing (Cai et al., 2019; Caulfield, 2009; Yu et al., 2017), which is good to endorse the new mobility paradigm but clearly not sufficient to support detailed policymaking regarding transportation environmental issues. Detailed and targeted policies require refined emission estimation at, e.g., road segments-level such as in (Hu et al., 2019) rather than overall aggregation. Furthermore, current literature has widely proved that ridesharing can mitigate traffic congestion and thus promote travel speed, but few studies has analyzed how this speed acceleration effect may further promote emission reduction, which is highly possible because it is well known that vehicular emissions are affected by driving conditions (Shang et al., 2014; Cai et al., 2019).

More importantly, all types of shared mobility *per se* are not sufficient to achieve the benefits. Any trips that meet each's travel requirement such as delay tolerance and time window could be pooled but may not reduce any VMT and emissions. Rather, the pooling solution should be integrated with optimization models and analytical tools that can evaluate the potential benefits (Santi & Ratti, 2017). Assessments that omit some critical requirements of urban trips (such as time window and delay tolerance) or are based on non-optimized ridesharing solutions may provide varying estimation as the sharing condition changes, making them inappropriate for supporting policymaking. Using real records derived from developing ridesharing market may also create biases. For example, on-demand ridesharing service has only been operated by Didi since November 2019, which does not allow the derivation of significant statistics, and thus may cause an underestimation of the environmental impacts as estimated by the scaling law of shareability reported in (Tachet et al., 2017).

Therefore, we argue that further evaluation is needed, which should be able to answer that (1) to which extent the traffic emission can be reduced by large-scale ridesharing rather than occasional orders, (2) what is the *upper bound* estimate of ridesharing's environmental benefits considering travelers' critical requirements and optimization models, and (3) how the speed fluctuations as well as ridesharing's speed acceleration effect can further affect the emission in ridesharing scenarios.

This paper endeavors to fill these gaps. First of all, using taxi data as a proxy of the ridesharing demand, potential shareability among 350,000 daily trips in Shanghai is explored based on the *Shareability Network* approach (Santi et al., 2014b), which can calculate the optimal matching of rides according to different optimization criteria so that the *upper bound* of ridesharing's environment benefit can be well estimated. Secondly, traffic emissions of each vehicle on each road are estimated by combining real traffic speeds and vehicle dynamics in the COPERT III model (Ntziachristos et al., 2000), so that the spatiotemporal patterns of emission reductions can be further analyzed at the street-level. Moreover, a speed-density traffic flow model is implemented to evaluate additional emission reductions provided by ridesharing's speed acceleration effect, i.e., traffic is reduced in large-scale ridesharing, and hence average vehicle speed on the roads is increased.

The paper is organized as follows: Section 2 provides a brief literature review of ridesharing's potential environmental benefits and traffic emission estimation models. In Section 3, the research framework is presented, under which the *Shareability Network* approach, the COPERT III model, the speed-density model, and the taxi data are introduced. Section 4 illustrates the overall emission reductions provided by ridesharing *per se* and by its first-order speed effect on traffic speeds, the spatial and temporal patterns of emission reductions, and the emission redistribution issue. Finally, a conclusion and policy implications are further discussed in Section 5.

2. Literature review

2.1. The potential environment benefits of ridesharing

To develop public policy regarding emerging shared mobility such as ridesharing, we need to first understand its potential impact. Early studies have evaluated the benefits of ridesharing with Shared Autonomous Vehicles (SAVs). For example, a case study in Singapore (Spieser et al., 2014) found that a shared-vehicle mobility solution could meet the personal mobility needs of the entire population with a fleet size approximately 1/3 of the total number of passenger vehicles currently in operation. Fagnant and Kockelman (2018) investigated SAVs' potential for U.S. urban areas via multiple applications in Austin. They confirmed that as the trip-making intensity rose and sharing parameters were loosened (such as users become more flexible in their trip timing), higher ridesharing percentages and less relocation helped reduce net VMT. Another study in New Jersey found that trips during peak hours had substantial ridesharing potential that would correspondingly decongest roadways while delivering excellent mobility with reduced energy and environmental consequences (Zachariah et al., 2014). A report titled *A New Paradigm for Urban Mobility* by the International Transport Forum (2015) also concluded that ridesharing is expected to reduce up to 90% of on-road vehicles, nearly double the average occupancy, thereby reducing at least 18% of total VMT and 30% of carbon dioxide emissions. Another agent-based simulation also found a similar reduction in travel time and fare (Martinez et al., 2015). The problem is that (1) these models were generally detached from realistic ridesharing because they failed to incorporate users' travel requirements such as time window and delay tolerance, and (2) the ridesharing solution is sometimes not optimized so that the benefits could vary dramatically as the experiment settings change.

Progresses have also been made in terms of benefits evaluation in more realistic ridesharing simulations. To solve the problem of computation and enable large scale evaluation, Santi et al. (2014b) introduced the *Shareability Network* approach that allows researchers to model the collective benefits of large-scale ridesharing as a function of passenger inconvenience. Applying this framework to taxi data in New York City, they found that with increased but still relatively low passenger discomfort, cumulative Vehicle-Miles-Traveled (VMT) could be cut by 40% and 30% in an ideal scenario and a more realistic scenario, respectively. By generalizing the shareability network to real-time high-capacity pooling, another study (Alonso-Mora et al., 2017) found that 98% of the current taxi rides could be served with just 3000 taxis of capacity four, and the number of required vehicles could be even smaller if capacity increases. The shareability network also applies for dynamic ride-sourcing, showing a considerable saving of vehicles (Vazifeh et al., 2018). The *Shareability Network* approach has various advantages, including computational efficiency, realistic scenario modeling, and upper bound estimation of the ridesharing benefits, which make it well fitted to our goals of this paper.

Since the environmental impacts of traffic are tied to per-kilometer emissions, the aforementioned studies generally assume that the benefit of ridesharing, no matter with self-driving fleets or a smart centralized operation platform, comes with reductions in service cost, emissions, and with split fares as well. Some case studies have also quantified the overall emission reductions provided by ridesharing. Drawing on raw observed ridesharing trip data provided by the Didi Chuxing company in China, Yu et al. (2017) found that the annual direct environmental benefits of ridesharing amount to about 46.2 thousand tons of CO_2 and 253.7 tons of NOx in Beijing. The problem is that at that time, the service provided by Didi at that time (in Chinese, "顺风车") was not on-demand ridesharing service (in Chinese, "拼车"). Rather, it serves mainly long-distance trips that have reservations in advance. Using taxi data, another study (Cai et al., 2019) quantified the potential benefits of ridesharing in Beijing and found that 33% of VMT and a massive amount of pollution emission could be reduced if ridesharing was implemented for the entire taxi fleet. However, their estimation could be significantly overestimated because they didn't take into account the time window parameter in ridesharing which reduces the possible pairs of shareable trips. Moreover, their analysis, as well as in other studies (Xue et al., 2018; Yin et al., 2018), only briefly reported the *overall* reduction rather than spatiotemporal patterns of the benefits. We believe the latter would be more critical for targeted policymaking.

We contend that knowing the overall benefit is insufficient for policymaking, considering the inevitable and natural spatial heterogeneity of the expected benefits. For instance, theoretical modeling suggests that shareability (the fraction of trips that can be shared) is heavily dependent on some key factors such as spatiotemporal trip density and traffic speed (Tachet et al., 2017), which are rarely homogeneous in urban space. Even streets within the same districts where travel requests are relatively dense may have dramatically different levels of emission reduction. Transportation-related policies such as right-of-way rules generally differ according to road attributes. Targeted policies require a deep understanding of the spatiotemporal patterns of ridesharing's environmental benefits.

2.2. Traffic emission estimation

Traffic emission can be estimated in mainly two levels: macroscopic and microscopic. Macroscopic models use aggregate methods to analyze the total emissions in spatial units based on average speed and fixed emission factors. Microscopic models, by contrast, generally use agent-level models to estimate the traffic emissions of each vehicle on each road-segment or intersection with dynamic emission factors calculated using speed fluctuations.

The COPERT III model (Ntziachristos et al., 2000) is a typical microscopic model designed to estimate the emissions of vehicles that meet the European emission standards. The COPERT III model has been calibrated and validated by (Shang et al., 2014; XIE et al., 2006) based on actual categories, driving cycle, and fuel characteristics of Chinese vehicles, providing valid equations for calculating dynamic emission factors, and has been implemented in many studies (e.g., Sun et al., 2018). There are alternative microscopic models with usually fixed emission factors. For example, Xue et al. (2018) utilized fixed emission factors obtained from the Integrated Energy and Environment Policy Assessment model for China (2016) model groups. Cai et al. (2019) calculated the emission reductions provided by ridesharing with fixed parameters provided in (Huo et al., 2009). However, using fixed emission factors and ignoring the effect of traffic speed may significantly underestimate the emissions because vehicles generally produce a lot more emissions when idling in congestion.

To estimate traffic emissions with dynamic factors, the traffic speeds must be known with high spatiotemporal precision. Emerging information and communication technologies and big data mining methods (Calegari et al., 2016; Lécué et al., 2014; Togawa et al., 2016) have improved the measurements of vehicle emission estimation, laying a solid foundation for relevant analysis. Researchers use spatiotemporal records provided by taxi GPS data to measure vehicle emissions, significantly improving measurement accuracy (Ibarra-Espinosa et al., 2020; Li et al., 2019; Liu et al., 2019).

3. Methodology and data

3.1. Research framework

This paper quantifies emission reductions provided by ridesharing in four steps. Specifically, we first infer Origin-Destination pairs from taxi data, which is a reliable proxy to the potential users of an on-demand ridesharing service. The original traffic speed on each road segment is extracted from the same taxi trajectory data (detailed in Section 3.5). Combining the original ODs, the original speeds, and the COPERT III model, the dynamic *original* traffic emissions are estimated (Section 3.3).

Then, by assuming that all the taxi ODs are willing to pool, we calculate the optimal ridesharing solution that has the largest overall

VMT reduction by using the *Shareability Network* approach. After that, combining the maximal solution and the road-specific speeds in the COPERT III model, we estimate the second result of dynamic traffic emission in two ridesharing scenarios — the *oracle* and *online* scenarios (Section 3.2). The former scenario models a situation in which daily ridesharing demand is known in advance and can be considered an *upper bound* to the emission reductions that could be achieved with increasingly accurate demand prediction technology. The latter models a situation in which only the ridesharing demand for the next few minutes is known, and it is more representative of the current ridesharing technology.

Thirdly, with a speed-density model, we estimate the first-order effect of ridesharing on the traffic speeds (Section 3.4). As also suggested in (Tachet et al., 2017), we can expect that if ridesharing reduces a large fraction of the VMT and on-road vehicles, the average traffic speed on road should go up, which may further reduce emissions. After the traffic speeds under ridesharing scenarios are estimated using the speed-density model, we calculate the third result of dynamic traffic emissions (Section 3.3).

Finally, comparing all the emission estimation, we calculate the emission reductions provided by ridesharing *per se* and its first-order speed effect, respectively. Both the overall and the spatiotemporal distribution of the emission reductions at each road segment are further analyzed. The detailed methodology is represented in Fig. 1 and discussed in the following.

3.2. The Shareability Network approach

We achieve the ridesharing functionality by incorporating a well-established shareability network (Santi et al., 2014b). A *Shareability Network* is a graph $G(V, E, W)$ in which every node T_i in $V = \{T_1, \cdots, T_n\}$ denotes one trip, every link T_{ij}^{share} in E represents a route that can serve two *shareable* trips via ridesharing, and each weight W_{ij} represents the weight of corresponding shared trip T_{ij}.

Whether the trips are *shareable* is determined as follows. Let $T_i = (o_i, d_i, rt_i^o, ct_i, pt_i^o, pt_i^d)$, $i = 1 \ldots k$ be k trips in a successfully combined/pooled trip where o_i and d_i denote the origin and destination of trip i, rt_i^o is the request time, ct_i is the delivery time without ridesharing, and pt_i^o, pt_i^d are the pick-up and drop-off times in the shared route T_{ij}^{shared}, respectively. The k trips are *shareable* if and only if there exists a route connecting all o_i and d_i in any order where each o_i precedes the corresponding d_i, except for configurations where single trips are concatenated and not overlapped like $o_1 \to d_1 \to o_2 \to d_2$, such that each passenger is picked up and dropped off at their respective origin and destination locations with delay at most Δ. Imposing a bound of k implies that only k trips can be shared using a taxi of corresponding capacity. This paper only focuses on the case of $k = 2$, considering that (1) the computation of $k \geq 3$ is only heuristically feasible or even intractable, and (2) even $k = 2$ can provide immense benefits to a dense enough community like New York City (Santi et al., 2014b).

In the case of $k = 2$, there are four possible pooling-routes: $o_i \to o_j \to d_i \to d_j$, $o_i \to o_j \to d_j \to d_i$, $o_j \to o_i \to d_i \to d_j$, and $o_j \to o_i \to d_j \to d_i$. With all trips put into G as nodes, a link T_{ij}^{shared} is constructed if and only if any combined trip among the four routes can be found so that trip/node i and j are *shareable*, i.e., each's delay and departure time are constrained within some pre-set windows. Formally, the following constrains are satisfied:

$$rt_i^o \leq pt_i \leq rt_i^o + \Delta \tag{1}$$

$$rt_j^o \leq pt_j \leq rt_j^o + \Delta \tag{2}$$

$$\left(dt_i^d - pt_i^o\right) - ct_i \leq \Delta \tag{3}$$

$$\left(dt_j^d - pt_j^o\right) - ct_j \leq \Delta \tag{4}$$

$$\left|pt_i^o - pt_j^o\right| \leq \delta < \Delta \tag{5}$$

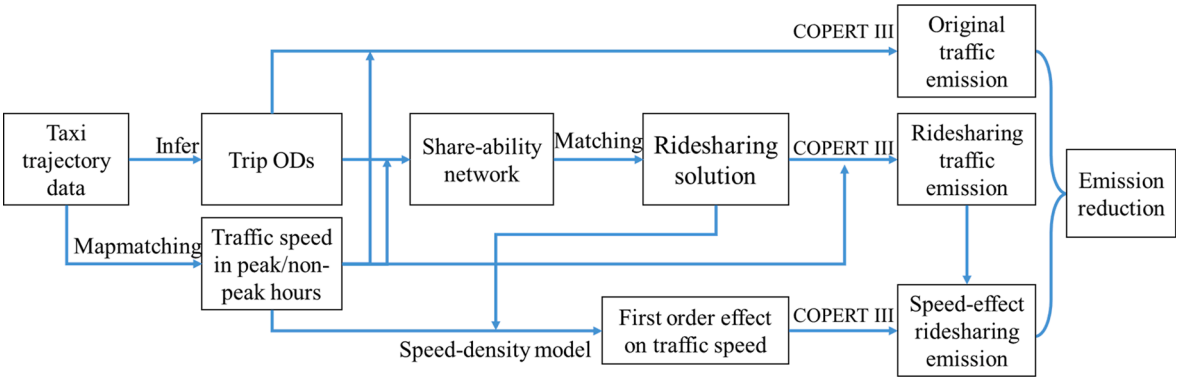

Fig. 1. Research methodology.

where pt_x and dt_x are the pick-up and drop-off times of trip x in the shared route T_{ij}^{share}; rt_x^o is the request time, and ct_x is the delivery time of trip x served by a single, individual trip — in this paper, it is set to the time cost of the path with the shortest travel time between o_x and d_x; and Δ is the pre-set maximum delay.

We estimate the benefits of ridesharing in two scenarios, i.e., with two different *time windows* δ. The time window δ is a parameter that reduces the possible pairs of T_{ij}^{share} in consideration. The *oracle* scenario assumes that all travel requests are issued in advance through a kind of reservation system, thus the possibility of sharing between any two trips will be exploited even if their starting times are separated by a relatively long time interval. For computation consideration, we set $\delta_{oracle} = 10min$. In contrast, the *online* scenario only considers travel requests initialed in a relatively short time window, which is more like a practical, real-time, on-demand ridesharing system. Following (Santi et al., 2014b), we set $\delta_{online} = 1min$.

Using the *Shareability Network* approach, classical algorithms for solving maximum matching on graphs (Cormen et al., 2009; Galil, 1986) can be used to determine the best solution according to different optimization criteria: *(a)* maximizing the number of shared trips — namely maximum cardinality matching, or *(b)* minimizing the cumulative time needed to accommodate all trips using maximum-weighted matching algorithms. This paper focuses on criterion *(b)*, considering that criteria *(a)* only provides proxy for the reduction in number of circulating taxis, while other important objectives such as minimizing Vehicle-Miles-Traveled (VMT) and emissions can be best approximated with *(b)*. Therefore, the integer programming model that solves the maximum-weighted matching is,

$$\min \sum_i \sum_j L_{ij} W_{ij} \tag{6}$$

$$s.t.\ \ Eq(1) - (5)$$

$$W_{ij} = \min_{M=4} \left(dt_m^{d\_share} - pt_m^{o\_share} \right) \tag{7}$$

where L_{ij} is the binary decision variable which equals to 1 when trip i and j are selected for sharing and equals to 0 otherwise; $pt_m^{o\_share}$ and $dt_m^{d\_share}$ are the pick-up and drop-off times of the whole shared route T_{ij}^{share}; and W_{ij} is the link weight on T_{ij}^{share}, which is set to the best choice of the four possible pooling-routes that has the minimum travel time to accommodate the combined trip of i and j, i.e., in the case of $k = 2$, $M = 4$.

Eventually, all trips are assigned to routes according to the optimized solution, based on which the VMT, hence, emissions, in case or ridesharing are calculated. The so obtained estimated emissions are then compared to those obtained in the original situation without ride sharing, so that the expected environmental benefits of ridesharing can be analyzed.

3.3. Estimation of traffic pollution emission

The COPERT III model (Ntziachristos et al., 2000) is used to estimate traffic pollution emissions. Although it may slightly overestimate the emissions because vehicular emission in China has followed more stringent emission standards since 2013, the model and parameters have been proved effective in Chinese cases (Shang et al., 2014; XIE et al., 2006). In the COPERT III model, traffic emissions consist of three parts: hot, cold start, and evaporative emissions. Hot emissions occur when the engine is at its normal regime, which is the general condition for a running vehicle and thus is our major concern. Cold start emissions denote emissions from transient engine operation, and evaporative emissions come from refueling and temperature changes. Following (Shang et al., 2014), the latter two parts are omitted in our estimation due to lack of data. They are also of less significance in terms of overall emissions (Gühnemann et al., 2004). The hot *emission factor* (*EF*) of a specific pollutant k, the amount of pollutant k a single vehicle emits per kilometer (g/km), is calculated as a function of travel speed$v$ (km/h) with five parameters a, b, c, d, and e:

$$EF_k = \left(a_k + c_k v + e_k v^2 \right) / \left(1 + b_k v + d_k v^2 \right) \tag{8}$$

The *emission factor* for some pollutants are given in Table 1. As for other pollutants like CO_2 and $PM_{2.5}$, their *emission factors* are fully proportional to FC (fuel consumption). For instance, the conversion factor for CO_2 and $PM_{2.5}$ are 3.18 and 3×10^{-5}, respectively.

$$EF_{CO_2} = 3.18 \times EF_{FC} \tag{9}$$

$$EF_{PM_{2.5}} = 3 \times 10^{-5} \times EF_{FC} \tag{10}$$

Table 1
Pollution emission parameters in COPERT III model.

	a	b	c	d	e
CO (Carbonic Oxide)	71.7	35.4	11.4	−0.248	0
HC (Hydrocarbons)	5.57×10^{-2}	3.65×10^{-2}	-1.1×10^{-3}	-1.88×10^{-4}	1.25×10^{-5}
NO_x (Nitrous Oxides)	9.29×10^{-2}	-1.22×10^{-2}	-1.49×10^{-3}	3.97×10^{-5}	6.53×10^{-6}
FC (Fuel Consumption)	217	9.6×10^{-2}	0.253	-4.12×10^{-4}	9.65×10^{-3}

Finally, the cumulative emission on a road segment i is:

$$E_{it,k} = EF_k \times N_{it} \times Len_i \tag{11}$$

where N_{it} is the number of vehicles passing through road segment i in a certain time t, and Len_i is the length of segment i (km).

3.4. First-order effect of ridesharing on traffic speeds

Theoretically, since ridesharing reduces the emissions by cutting down the VMT, it may also alleviate congestion and increase traffic speeds by reducing the number of on-road vehicles, which may double back and further promote the shareability hence the emission reduction. In this paper, we only consider the first-order effect of ridesharing on traffic speeds and ignore any second or even third-order effects. We utilize a simple Speed-Density model (Hall, 1996), as it can infer the increase in speeds based on just the changes in traffic density. Specifically, denote u_0 as the free-flow speed, then the estimated traffic speed u in a specified length of road (veh/km) with a density of traffic stream k is,

$$u = -u_0 \ln\left(k/k_{jam}\right) \tag{12}$$

where k_{jam} is the jam density (veh/km). We set u_0 for each road segment as the median free-flow speed in the late night and before the morning peak so the improvement of traffic speed (Δu) could be directly calculated using $\delta_{RS}^{overall}$ — the ratio between the *overall traffic flow* density in ridesharing scenarios ($k_{RS}^{overall}$) and the original density ($k_{original}^{overall}$).

$$\Delta u = u_{RS} - u_{original} = -u_0 \ln\left(k_{RS}^{overall}/k_{original}^{overall}\right) = -u_0 \ln \delta_{RS}^{overall} \tag{13}$$

$$u_{RS} = u_{original} + \Delta u = u_{original} - u_0 \ln \delta_{RS}^{overall} \tag{14}$$

Then, denote the ratio of the *non-sharing* traffic flow density ($k_{original}^{non-share}$, which is the traffic flow of all vehicles except for the taxi fleet of this Qiangsheng company) to the traffic flow density of *sharing* vehicles ($k_{original}^{share}$, which is the traffic flow of the considered taxi fleet) as τ, and denote k_{RS}^{share} and $k_{original}^{share}$ as the traffic flow density of considered *shareable* vehicles in a *ridesharing scenario (RS)* and the *original* case, respectively, and assume $k_{original}^{non-share}$ remains the same in any *ridesharing scenario (RS)* and the *original* case, then the $\delta_{RS}^{overall}$ is calculated by,

$$\delta_{RS}^{overall} = \frac{k_{RS}^{overall}}{k_{original}^{overall}} = \frac{k_{RS}^{share} + k_{original}^{non-share}}{k_{original}^{share} + k_{original}^{non-share}} = \frac{k_{RS}^{share}/k_{original}^{share} + \tau}{1 + \tau} \tag{15}$$

where $k_{RS}^{share}/k_{original}^{share}$ simply represents the proportional change of the number of on-road shareable vehicles before and after ridesharing, which can be directly estimated using the *Shareability Network* model. Note that $k_{original}^{non-share}$ remains constant is a strong assumption, since ridesharing would surely change the overall traffic density hence traffic speed, which in turn lead to the difference in $k_{original}^{non-share}$. The assumption is made because the *non-sharing* traffic flow data is inaccessible for now. After obtaining the new speed in

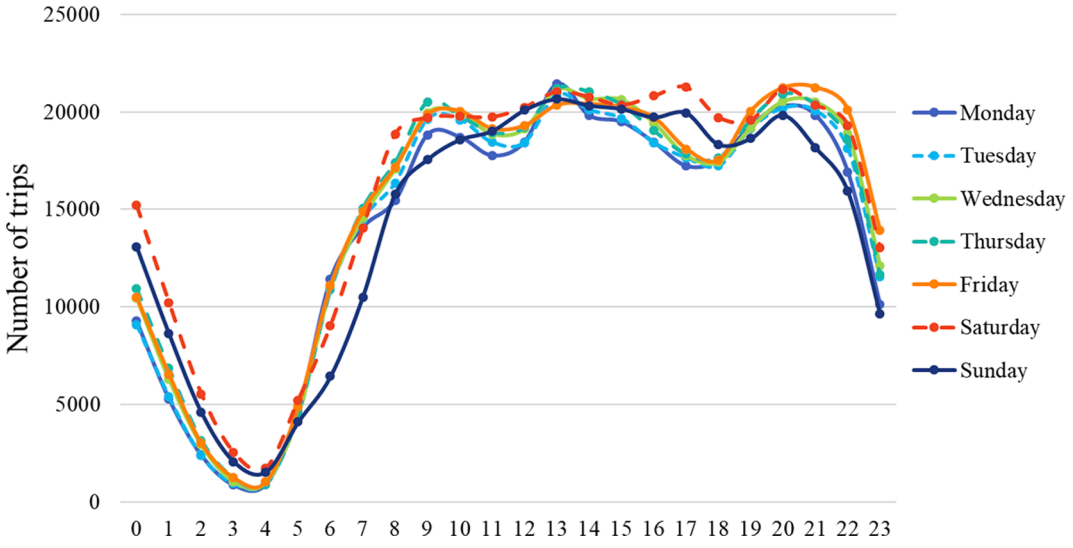

Fig. 2. Temporal distribution of taxi trips in a typical week.

ridesharing scenarios using Eqs. (13)–(15), the reduced emission can be estimated based on the methods in Section 3.3 using Eqs. (8)–(11) and parameters in Table 1.

3.5. Data and preprocessing

We utilized detailed taxi GPS trajectory data collected in April 2015 in Shanghai provided by Qiangsheng, the largest taxi company in Shanghai which has about 13 thousand taxi vehicles. The travel Origin-Destinations pairs are inferred using a Boolean field that constantly records whether there are passengers on board or not. The company serves about 350,000 trips per day, which varies between 300,000 and 400,000 on different weekdays. The temporal distribution of the taxi trips does not show significant peaks in the morning, noon, or evening (Fig. 2). To the best of our knowledge, this is probably because the supply of taxi services in Shanghai falls short of the demand during peak hours.

In this case, $\delta_{RS}^{share}$is estimated as follows. According to the Fifth Travel Survey of Residents (2009) and the Fifth Comprehensive Traffic Survey (2014) in Shanghai, only 6.6–7.0% of all trips are served by taxis, while 19.2–20.0% are served by private cars. The ratio between trips by private cars and all taxi vehicles is approximately 3:1. Since we only have the data of one company with a market share of about 25%, the ratio τ is given by the ratio of trips by private cars to the sharing vehicles (the considered Qiangsheng taxi fleet), i.e., $\tau = \frac{3}{1}\tilde{A} \cdot 25\% = 12$. Therefore, according to Eq. (15), the improved traffic speed on each road caused by the speed effect of ridesharing is:

$$u_{RS} = u_{original} + \Delta u = u_{original} - u_0 \ln\left(\frac{\left(12 + \delta_{RS}^{share}\right)}{13}\right) \tag{16}$$

The GPS location is updated every ten seconds, allowing for an accurate estimation of speed. We utilize the Hidden-Markov-Model (Newson & Krumm, 2009) to do the *Map-matching* task, i.e., to match the GPS trajectories to the road segments. Then, we select the median speed on each road segment in peak/non-peak hours and transform the speeds into *passing-through times* for further simulation. Peak hours are set to 7-9am and 5–7 pm, according to Amap's (one of the largest online map servicers in China, belongs to Alibaba) annual transportation report (2019). Finally, all the travel time in the *Shareability Network* construction process are calculated by implementing shortest paths algorithms (e.g., *Dijkstra*) over the road network weighted by the selected *passing-through time*.

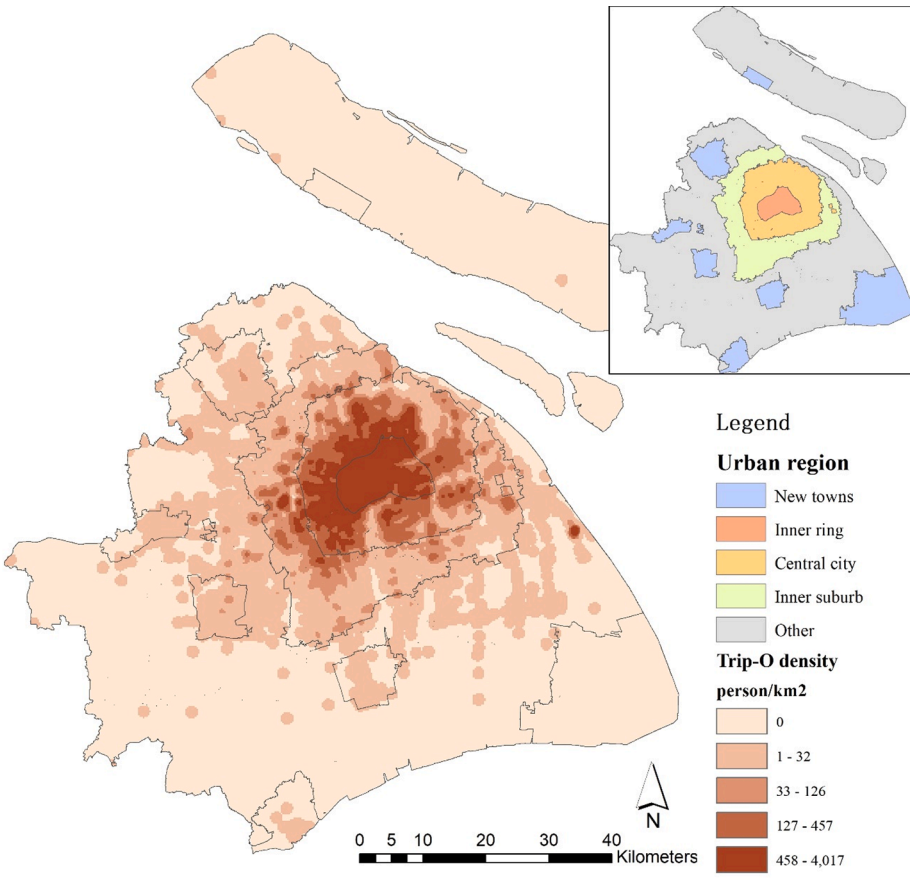

Fig. 3. Spatial distribution of daily trip origins in research area.

Our evaluation covers the entire administration area of Shanghai. The city can be divided into the inner ring area, the central city (inner ring included), the inner suburban area, the seven suburban new towns, and the remaining suburban area. The spatial distribution of the taxi trips explicitly demonstrates a monocentric structure with the density gradually declining from the inner ring to the suburban area (Fig. 3).

4. Results

4.1. Overall emission reductions from ridesharing

Our result highlights significant traffic emission reductions brought by ridesharing. As shown in Table 2, in *oracle* scenario, ridesharing saves 3695 tons CO_2, 1162 tons FC, 10.87 tons CO, 1.4 tons NOx, 0.32 tons HC, and 0.04 tons $PM_{2.5}$ emissions monthly. The savings in *online* scenario is about 66% of the *oracle* numbers. With quite a close scale of trips and taxi fleets, our estimations are much smaller than those found in the Beijing case (Cai et al., 2019), which claimed that ridesharing could save 199 tons CO, 16.5 tons NOx, 2.08 tons $PM_{2.5}$ monthly. There are three reasons: firstly as discussed in Section 2.1, they didn't take into account the *time window* parameter (δ) in ridesharing modeling; secondly, the delay tolerance in their paper is 10 min while we use 5 min; finally, as discussed in Section 2.2, their emission estimation used fixed *emission factors* and ignored the effect of traffic speed. Therefore, our estimation can be more reliable.

In contrast to the absolute quantities, the reduction percentage is more helpful to understand the benefits of ridesharing. In *oracle* ridesharing scenario, both VMT, FC, and all the polluting emissions drop by 22.88%–23.31%. Among all the pollutants, NOx has the largest reduction (23.25%), followed by CO > FC/CO_2/$PM_{2.5}$ > HC (22.54%). The deviation is only 0.7%, indicating that the emission reductions due to ridesharing are generally close regarding different pollutants. In the *online* scenario, since shareability between trips is limited by a relatively short *time window*, the reduction percentages decline by about 7.8% from the *oracle* scenario, ranging from 14.78% to 15.44%. This is reasonable because smaller *time window* significantly reduces the "edges" in the shareability network, i.e., the possible combinations of ODs that are *shareable*. Ridesharing between many ODs is therefore infeasible in time, even if the sharing may reduce a lot of VMT. The observed reduction in emission between *oracle* and *online* scenario is consistent to the VMT reduction observed for the New York case (Santi et al., 2014b), in which the VMT reduction percentages in *online* scenario drops about 10% from the *oracle* scenario.

Ridesharing's first-order speed acceleration effect can additionally promote a small but considerable emission reduction. In Table 2, the columns marked with "delta" refer to the additional emission reductions due to ridesharing's speed effect compared to only ridesharing ("Oracle/Online-RP"). It demonstrates that in addition to CO, emissions of other pollutants and FC are all further reduced by 0.36–0.96% in *oracle* scenario and 0.34–0.74% in *online* scenario. Even though the number is small, the real improvement is still considerable since the speed effect is spontaneous, that is to say, as long as ridesharing mitigates on-road traffic flow to the same extent as in our modeling result, its speed acceleration effect will very likely to further reduce that much emissions. Furthermore, the difference between the additional savings in *oracle* and *online* scenarios is surprisingly small (0.02–0.22%, except for CO), especially when compared with the aforementioned difference in the overall percentage (7.8%), indicating that the two scenarios may perform similarly in terms of the speed effect as well as the VMT reduction for some of the most congested roads.

Moreover, the additional savings provided by ridesharing's speed effect are ordered as FC/CO_2/$PM_{2.5}$ > NO_x > HC > CO, which could be explained by the *emission factors*. More specifically, according to the COPERT III model and as shown in (Luo et al., 2017), the *emission factors* of FC/CO_2/$PM_{2.5}$ and NO_x always diminish when speed increases under 100 km/h, and the *emission factors* of HC and CO only decrease when speed increases under 60 km/h and 30 km/h, respectively. Therefore, on some roads with traffic speeds exceeding 60 km/h and 30 km/h, the *emission factors* of HC and CO — the pollution a vehicle emits per kilometer — grow as traffic speeds increase. Since realistic traffic speeds are usually above 30 km/h, the cumulative emissions of CO increase noticeably along with the positive effect of ridesharing on traffic speeds.

Table 2
Cumulative emission and ridesharing reduction over 30 days.

Pollutant	Cumulative emission			Reduction Percentage (RP)				Additional reduction	
	Original	Oracle	Online	Oracle-RP	Online -RP	Oracle-RP1st	Online -RP1st	Oracle-delta	Online-delta
VMT (10^6km)	81.860	62.780	69.192	23.31%	15.48%				
CO (t)	47.179	36.309	39.998	23.04%	15.22%	21.76%	14.33%	−1.28%	−0.89%
HC (t)	1.434	1.110	1.222	22.54%	14.78%	22.90%	15.12%	0.36%	0.34%
NO_x (t)	6.011	4.613	5.083	23.25%	15.44%	24.00%	16.01%	0.75%	0.57%
FC (10^3t)	5.078	3.916	4.312	22.88%	15.09%	23.84%	15.83%	0.96%	0.74%
CO_2 (10^3t)	16.148	12.453	13.711	22.88%	15.09%	23.84%	15.83%	0.96%	0.74%
$PM_{2.5}$ (t)	0.152	0.117	0.129	22.88%	15.09%	23.84%	15.83%	0.96%	0.74%

Note: The "RP" refers to the reduction percentage provided by ridesharing compared to original emissions. The "1st" refers to the reduction percentage taking into account the first-order speed effect. The "delta" refers to the additional reduction between "RP" and "1st".

4.2. Spatial patterns of the emission reduction

Understanding the spatial and temporal characteristics of the emission reductions is crucial for public policymaking. Since the spatiotemporal patterns of different pollutants are generally similar, we use fuel consumption (FC) as an example for further analyses.

Notably, the reductions of traffic emission are more significant at severely polluted locations, following something like the *Matthew Effect*. Fig. 4 depicts the cumulative FC in ridesharing scenarios against the original FC aggregated by road segment. On the most polluted roads where the monthly cumulative FC is higher than 10 tons, ridesharing can reduce 35% and 27% of the emission in *oracle* and *online* scenario, respectively, which are significantly larger than the overall average reduction percentages. The linear regressions between the cumulative FC in ridesharing scenarios against the original FC shows that both the R-squared values are quite close to 1, indicating that the *Matthew Effect* is generally stable for both scenarios. Meanwhile, the *online* scenario does have relatively smaller emission reductions and a weaker linear pattern due to the reason described in Section 4.1.

This spatial *Matthew Effect* is also effective in emission reductions provided by ridesharing's first-order speed effect, but is weaker with smaller R-squared values. Fig. 5 depicts the additional FC reduction due to the speed effect against the cumulative original FC. It shows that the linear relationship, i.e., more original FC, more FC reduced by the speed effect, is distinct on the busiest streets, such as those with original FC larger than 12 tons. Many of the average roads have relatively small additional reductions. This is probably because ridesharing's speed acceleration effect is not evenly distributed and mainly happens on the most congested roads.

Taking the *oracle* scenario as an example (the *online* scenario is fairly similar), we map the cumulative original FC, reduced FC, and additional reduction due to speed effect in Fig. 6. The result shows two distinct patterns, indicating explicit connections between the urban spatial structure of Shanghai and emission savings.

The first pattern is a monocentric and concentric structure of the city, which can be easily explained by the spatial aggregation of trip origins, as shown in Fig. 3. Specifically, both the original FC (Fig. 6a) and the direct emissions reduction (Fig. 6b) concentrate in the inner ring area and generally decay futher out. Statistics show that the average *oracle*-RP values in the inner ring and central city are as high as 28.38% and 23.04%, respectively, while the average percentage in the suburban area is only 2.24%. In general, as reported in Table 3, both reduction percentages and additional savings due to the speed effect for both scenarios exhibit this monocentric and concentric pattern. Furthermore, although the new towns do have much higher reduction (7.14%) compared to the average suburban area, their numbers are much smaller than the inner suburban area (13.91%), following the monocentric pattern once again. In fact, such a structure of Shanghai has been revealed in many transportation studies (Yan et al., 2019).

The second pattern is the highlighted circular and radial trunk roads with a relatively high concentration of original FC as well as pollution emissions. These roads also have significantly higher reduction percentages than other roads. In contrast, some of the local grid roads have moderate original FC as well as reduction percentages; and the branch roads, even many of those inside the central city or inner ring area, have the lowest reduction percentages (Fig. 6). This pattern can be explained by the grading and topology of the roads — because the circular and radial trunk roads are more often used in individual routes (i.e., have higher trip-weighted betweenness centrality), the VMT, hence emission, on them are more likely be reduced when trips are shared.

Moreover, the additional benefit generated by the speed effect also demonstrates similar patterns, including the monocentric structure, the highlighted circular and radial trunk roads, and the local grid roads. The difference is that additional reduction is more heterogeneously distributed and more spatially concentrated in space. In Fig. 6c, speed effect can reduce cumulative FC by more than 10 kg on most of the circular and radial trunk roads inside the central city, which is equivalent to the direct reduction on the orange roads in Fig. 6b. This is because the roads with the highest FC are also the most congested, thus more likely to have speed increases due to ridesharing. In contrast, the additional reductions on the branch roads, even those within the central city, are comparatively small due to less speed gains.

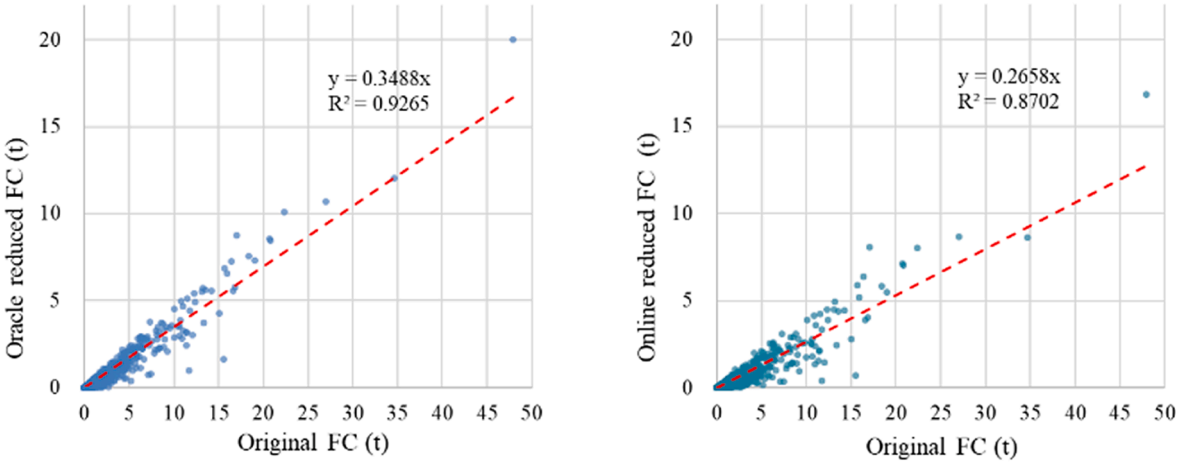

Fig. 4. FC aggregated by road segment: original FC versus reduced FC by pooling: *oracle* (left) and *online* (right) ridesharing scenario.

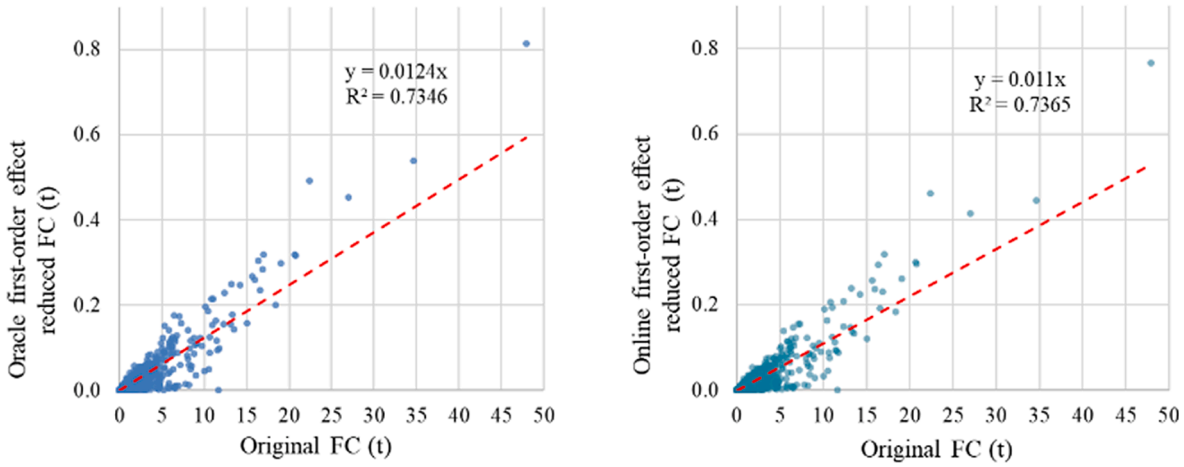

Fig. 5. FC aggregated by road segment: original FC versus additional reduced FC due to the speed effect: *oracle* (left) and *online* (right) ride-sharing scenario.

4.3. Temporal patterns of the emission reduction

Our temporal analysis shows that the emission reductions provided by ridesharing are considerably stable over time. Fig. 7 depicts the hourly variation in FC and the ultimate reductions due to ridesharing and the speed effect in different scenarios. The original FC plot has four distinct peaks: an intensive morning peak in 7-9am and three moderate ones in 12am-1 pm, 3–4 pm, and 7–9 pm. The evening peak is about 2 h later than the one presented in Amap's report (5–7 pm), which may be because taxi drivers in Shanghai used to change shifts at round 5 pm, making the service supply much less than real demand. Regardless of these fluctuations, after 9am, the emission reduction percentages are generally stable at 25% and 17% for *oracle* and *online* scenarios respectively, with a deviation smaller than 1%. Eventually, the emission reduction percentages drop from midnight to 4am and stay at a low level until 6am, as there are few passengers through that time.

The hourly spatial mapping further demonstrates how the spatial patterns shifted between organized and disorganized structures. Fig. 8 depicts the spatial distribution of FC and *Oracle* reduction percentage (with the first-order speed effect) for three typical 2-hours within the central city. The 4-5am period is an example of the early morning (Fig. 8a). Since trips in this period are mainly dispersed early commuting, both the concentration of original FC and the reduction percentages are disorganized. Traffic emissions on most of the branch roads within the central city generally remains unreduced. Hence, significant ridesharing reduction happens occasionally at fragmented road segments, suggesting that there is no association with original FC.

In contrast, the 7–8 am period represents the four peaks when trips and the original FC agglomerate spatially (Fig. 8b), emphasizing the two aforementioned spatial patterns in Section 4.2. Since this time period only includes two hours, the spatial pattern of the highlighted roads here is slightly more fragmentary than that in Fig. 6b. However, the monocentric and concentric structure and the highlighted circular and radial trunk roads are distinct: the reduction percentages gradually decline from the inner ring area out to the suburban area, while most of the trunk roads benefit significantly from ridesharing.

The 10–11 pm period represents a non-peak segment during a day (Fig. 8c). Although the original FC is distributed in almost the same way as the 7–8 am, a lot more disorganization can be seen with respect to the spatial patterns of the reduction percentages. Specifically, quite a few branch roads in the inner city and even some trunk roads drop one or two reduction levels, making both the monocentric structure and the circular and radial pattern less evident. The overall spatial pattern becomes more like a state in between organized and disorganized.

4.4. Redistribution of traffic emission: Some environmental injustice discussion

There is another finding worth discussion: not only are the emission reductions uneven across the city, the emissions even increase at some locations, thus creating a new environmental injustice issue. In our static shareability model, such injustice may be relative rather than absolute. Specifically, in Fig. 9-left, when O_1D_1 and O_2D_2 are served by combined routes (the dashed route) instead of individual routes (solid routes), the green part is reduced by ridesharing and modeled, the orange parts are also reduced but not modeled, and the emissions on red roads are modeled to be increased. Taken together, ridesharing in our model may increase the traffic emission on the red segments, which, however, may not happen for dynamic ridesharing in the real world since when aggregated together, the orange part may *offset* the red part. Additionally, this also indicates that our static shareability model may underestimate the benefit of emission reductions provided by ridesharing at a certain extent because we do not model the reduced passenger searching, i.e., the orange parts.

If the *offset* does not occur, i.e., the environmental injustice does appear, it will firstly appear on the red roads as revealed in our model. Nevertheless, such environmental injustice will be quite limited. Fig. 9-right is a plot of the zone surrounding the zero-point in

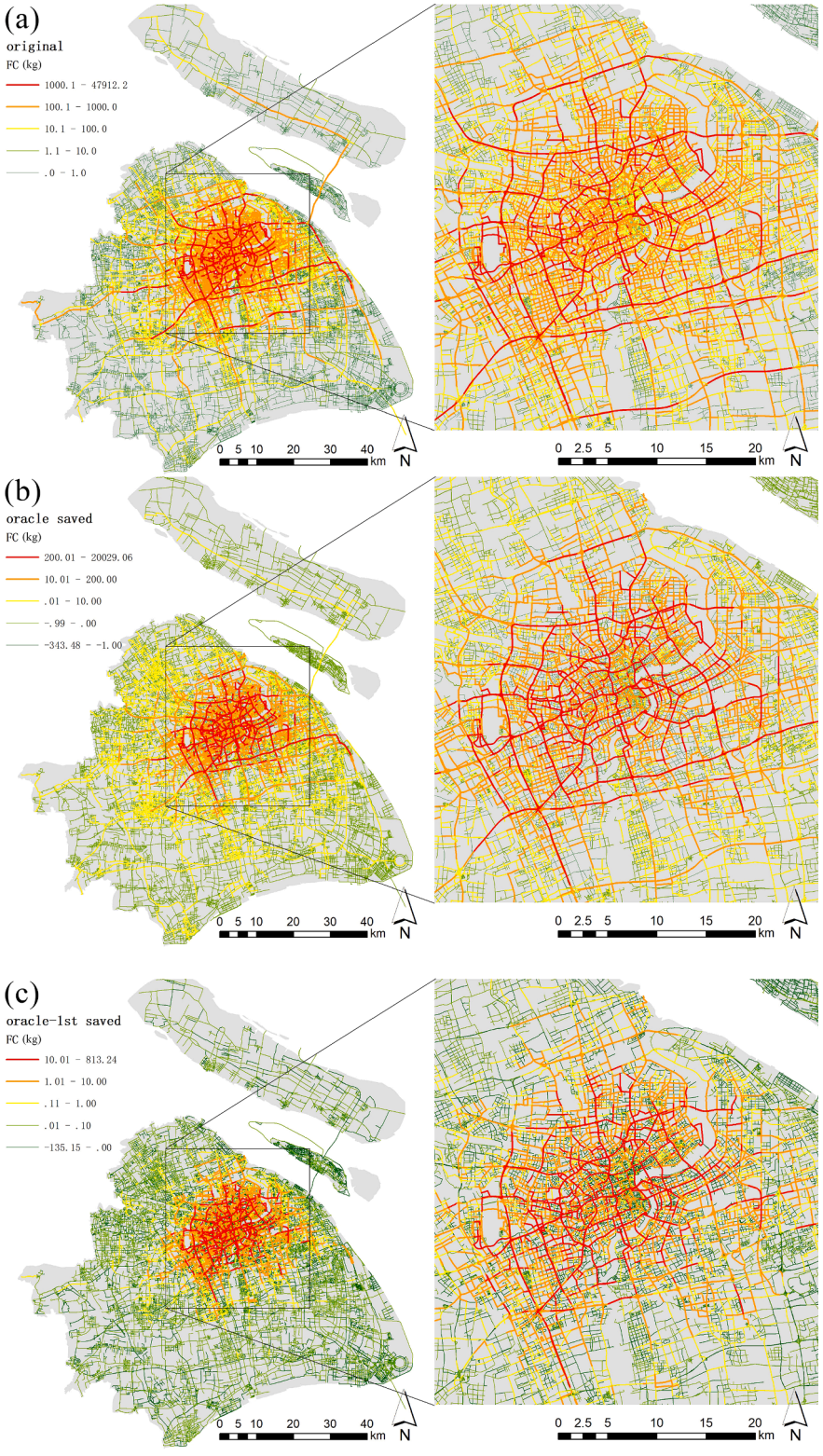

Fig. 6. Cumulative original FC (a), reduced FC in *Oracle* scenario (b), and additional reduced FC (c) due to ridesharing's speed effect in *Oracle* scenario.

Table 3
Cumulative emission and pooling reduction aggregated by regions.

Spatial division	Reduction Percentage		Additional reduction	
	Oracle-RP	Online-RP	Oracle-delta	Online-delta
Inner ring	28.38%	20.37%	1.30%	1.08%
Central city (inner ring excluded)	23.04%	14.70%	0.93%	0.69%
Inner suburban area	13.91%	7.44%	0.49%	0.31%
Suburban area (new towns excluded)	2.24%	0.94%	0.17%	0.10%
Suburban new towns	7.14%	3.15%	−0.01%	0.01%

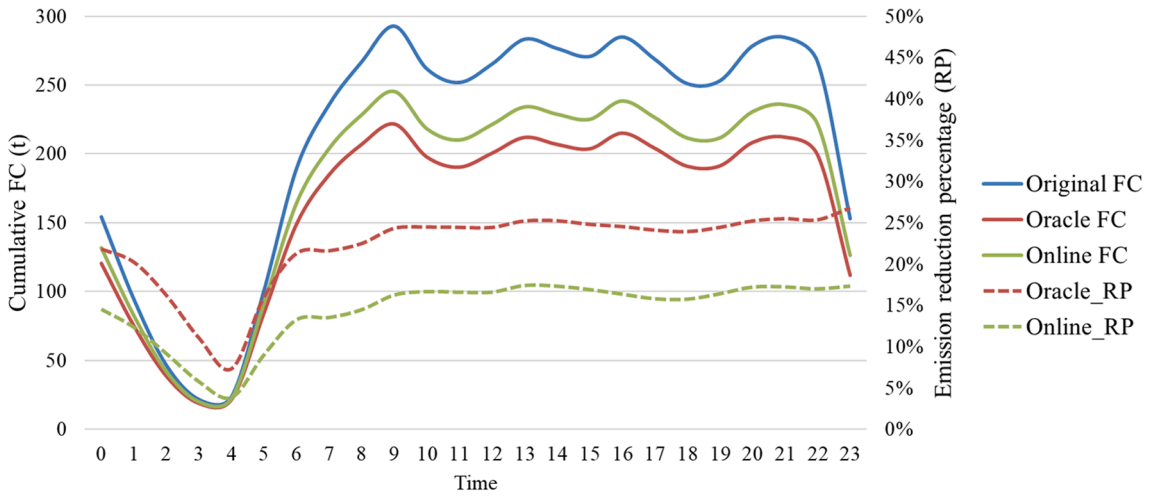

Fig. 7. Hourly FC and reduction percentages.

Fig. 4-left and highlights the increased FC (i.e., negative reduced FC) versus original FC. It shows that the 30-days cumulative increase in FC is 0.18tons at most, which makes the environmental injustice issue less significant than expected. Moreover, such environmental injustice only exists on the roads with relatively small original FC, i.e., mostly the branch roads. The reason is that high level roads (mostly circular and radial trunk roads) are more likely to be part of the shortest paths, which can be reduced by ridesharing just as the green part in Fig. 9-left. On the contrary, it is more likely for branch roads to play the role of the red part rather than orange or green parts, making their cumulative emissions sometimes increase. This indicates that if ridesharing in the real-world was to cause such environmental injustice, the transportation-environmental policy needs to pay more attention to the minor streets.

5. Conclusions, discussion, and policy implications

5.1. Conclusions and discussion

Based on the *Shareability Network* approach, the COPERT III emission model, the speed-density traffic flow model, and the detailed taxi trajectory data in Shanghai, this paper provides an accurate upper bound estimation of the environmental benefits of large-scale ridesharing as well as analysis of its spatiotemporal patterns. Several findings are obtained, which fill an essential gap in our understanding of the potential of emerging ridesharing services in megacities.

(1) Our results show that ridesharing is able to significantly reduce traffic emissions. Ridesharing *per se* can save 22.88% and 15.09% of the FC (fuel consumption) in *oracle* and *online* scenarios, respectively, and proportionally reduce traffic emissions. Here, the *online* scenario is very close to a real-time, on-demand ridesharing system that involves only a single taxi company, indicating that an emission reduction around 20% is highly possible as the market grows. The order of the pollutants in terms of reduction percentage is NOx > CO > FC/CO_2/$PM_{2.5}$ > HC.
(2) Moreover, ridesharing's first-order speed acceleration effect further reduces FC by 0.36–0.96% and 0.34–0.74% in *oracle* and *online* scenarios, respectively, which is small but considerable since the speed effect is spontaneous. For different pollutants, the additional benefits of HC and CO are significantly smaller than others, which can be explained by the relationship between their *emission factors* and the speed.
(3) Both ridesharing *per se* and its first-order speed effect reduce more emissions where the traffic is more polluting. This *Matthew Effect* leads to two spatial patterns for ridesharing's environmental benefits: (1) a monocentric and concentric structure and (2) a

Fig. 8. Spatial distribution of cumulative FC and *Oracle* reduction percentage in typical hours.

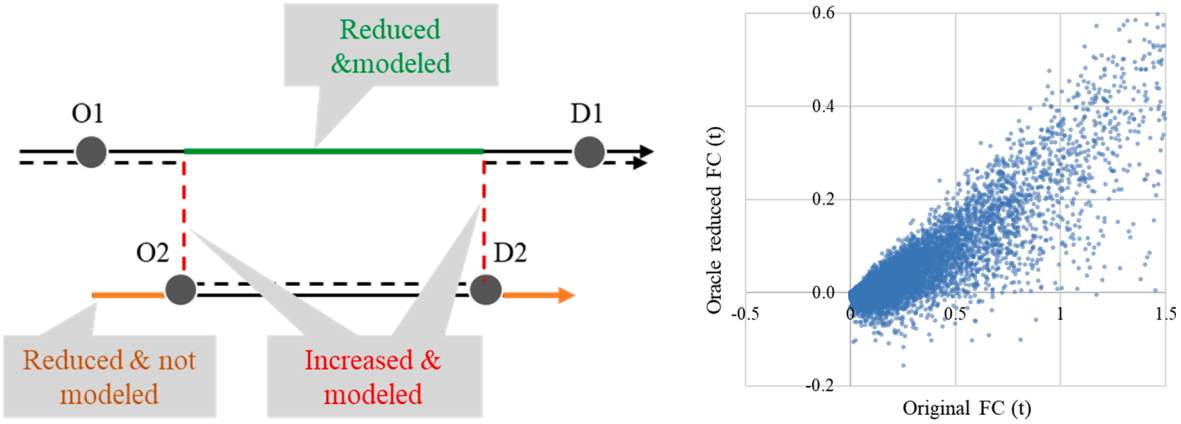

Fig. 9. The emission redistribution for combined routes (left) and the cumulative FC reduction nearby zero-point (right). In the right figure, the negative numbers of the reduced FC correspond to increased emissions due to ridesharing's redistribution effect in the left figure.

pattern following the circular and radial trunk roads, which can be explained by the spatial aggregation of trips and the grading and topology of the roads, respectively.

(4) Our temporal analysis shows that the emission reductions provided by ridesharing is considerably stable across time. The hourly spatial mapping further demonstrates that patterns shifted from disorganized to organized when the hourly spatial distribution of trips varies from dispersed to concentrated.

(5) Ridesharing may lead to increased emission at some small branch roads, and thus creating a new environmental injustice issue. Nevertheless, the 30-days cumulative increment of FC at these roads is only 0.18tons at most, which makes the environmental injustice less impactful than expected.

This study has several limitations. We failed to consider dynamic ridesharing scenarios in which vehicle dispatching and rebalancing are well simulated. We also failed to estimate the effect of speed change on the routing choices and emission of the private cars. And more analyses are needed to reveal the fundamental factors behand the spatiotemporal patterns.

5.2. Policy implications

We contend that a detailed evaluation of emission reduction performance should be part of the key criteria used to elaborate transportation-environment policies regarding ridesharing. Although ridesharing is shown to be environmental-friendly in this paper, the estimation based on the *Shareability Network* approach is more like a *reasonable upper bound* estimation. In the real world, ridesharing *per se* is insufficient to achieve the emission reduction goal. Rather, it should be designed to have emission reductions or related criteria as an explicit optimization goal. For example, any policy tries to promote either a casual sharing service provided by existing private drivers or formal services provided by the TNCs should be carefully evaluated in terms of how it can prompt environmental benefits — through changing users' behavior (such as increasing delay tolerance), transportation demand management (that affects the time windows in ridesharing), or operational strategies (such as the maximum-weighted matching solution). Therefore, this paper actually provides a framework to evaluate the environmental benefits of ridesharing services. By combining the models and data introduced in Section 3, the alternative policies and their effects on key parameters can and should be further modeled and evaluated before implementation.

In addition, our analyses strongly suggest that ridesharing related policies should be spatiotemporally targeted. The Shanghai case reveals three crucial dimensions: the spatial division, road grading, and different time periods. More specifically, we argue that in the early stages of ridesharing development, ridesharing promotion policies should be tentatively implemented in the densest urban regions, on the busiest roads, and during peak hours. For example, policies such as giving shared vehicles the same right-of-way as buses can be first implemented within the central city much like the current time-based traffic control policy that forbids foreign vehicles on elevated road during peak hours. On the contrary, the same level of emission reductions in suburban areas or the new towns will only be possible when the ridesharing market there has grown enough. Again, such policies can be well assessed by the methodology introduced in this paper.

Finally, our spatiotemporal analyses also imply the potential benefits of setting fixed pooling points on branch roads where travel requests may have priority over other locations. On one hand, pooling points can gather trip origins so that more trips may be *shareable*, creating more opportunities to achieve higher levels of shareability, hence leading to more emission reductions. On the other hand, considering one-way traffic is the typical situation regarding the branch roads in Shanghai, such pooling points can reduce the detour within communities, thereby alleviating potential environmental injustice discussed in Section 4.4.

Declaration of Competing Interest

The authors declare that they have no known competing financial interests or personal relationships that could have appeared to influence the work reported in this paper.

Acknowledgement

This study is supported by the National Key Research and Development Program of China (2018YFC0704600, 2018YFB1601301-3) and the National Natural Science Foundation of China (51838002, 51708414, 71890973, 71734004).

References

Alonso-Mora, J., et al., 2017. On-demand high-capacity ride-sharing via dynamic trip-vehicle assignment. Proc. Natl. Acad. Sci. 114, 462–467.
Brown, A., et al., 2014. An analysis of possible energy impacts of automated vehicle. Springer, pp. 137–153.
Cai, H., et al., 2019. Environmental benefits of taxi ride sharing in Beijing. Energy 174, 503–508.
Calegari, G.R., et al., 2016. City data dating: Emerging affinities between diverse urban datasets. Inform. Syst. 57, 223–240.
Caulfield, B., 2009. Estimating the environmental benefits of ride-sharing: A case study of Dublin. Transp. Res. Part D: Transp. Environ. 14, 527–531.
China Vehicle Environmental Management Annual Report, 2018. China Vehicle Environmental Management Annual Report. Ministry of Ecology and Environment of the People's Republic of China.
Cormen, T.H., et al., 2009. Introduction to algorithms. MIT press.
Fagnant, D.J., Kockelman, K.M., 2018. Dynamic ride-sharing and fleet sizing for a system of shared autonomous vehicles in Austin, Texas. Transportation 45, 143–158.
Galil, Z., 1986. Efficient algorithms for finding maximum matching in graphs. ACM Comput. Surv. (CSUR) 18, 23–38.
Gorham, R., 2002. Air pollution from ground transportation. An Assessment of Causes, Strategies and Tactics, and Proposed Actions for the International Community. United Nations, Division of Sustainable Development, Department of Economic and Social Affairs, New York.
Gühnemann, A., et al., 2004. Monitoring Traffic and Emissions by Floating Car Data. Institute of Transport Studies Working Paper.
Hall, F.L., 1996. Traffic stream characteristics. In: Traffic Flow Theory. US Federal Highway Administration, p. 36.
Hu, S., Chen, P., Lin, H., Xie, C., Chen, X., 2018a. Promoting carsharing attractiveness and efficiency: An exploratory analysis. Transp. Res. Part D: Transp. Environ. 65, 229–243.
Hu, S., Chen, P., Xin, F., Xie, C., 2019. Exploring the effect of battery capacity on electric vehicle sharing programs using a simulation approach. Transp. Res. Part D: Transp. Environ. 77, 164–177.
Hu, S., Lin, H., Xie, K., Chen, X., Shi, H., 2018b. Modeling users' vehicles selection behavior in the urban carsharing program. IEEE, pp. 1546–1551.
Huo, H., et al., 2009. Total versus urban: Well-to-wheels assessment of criteria pollutant emissions from various vehicle/fuel systems. Atmos. Environ. 43, 1796–1804.
Ibarra-Espinosa, S., et al., 2020. High spatial and temporal resolution vehicular emissions in south-east Brazil with traffic data from real-time GPS and travel demand models. Atmos. Environ. 222, 117136.
International Transport Forum, 2015. A New Paradigm for Urban Mobility: How Fleets of Shared Vehicles Can End the Car Dependency of Cities. Organisation for Economic Co-operation and Development.
Jin, S.T., et al., 2018. Ridesourcing, the sharing economy, and the future of cities. Cities 76, 96–104.
Lécué, F., et al., 2014. Smart traffic analytics in the semantic web with STAR-CITY: Scenarios, system and lessons learned in Dublin City. J. Web Semant. 27, 26–33.
Li, T., et al., 2019. Emission pattern mining based on taxi trajectory data in Beijing. J. Cleaner Prod. 206, 688–700.
Litman, T., 2013. Comprehensive evaluation of energy conservation and emission reduction policies. Transp. Res. Part A: Policy Pract. 47, 153–166.
Liu, J., et al., 2019. Spatial-temporal inference of urban traffic emissions based on taxi trajectories and multi-source urban data. Transp. Res. Part C: Emerg. Technol. 106, 145–165.
Luo, X., et al., 2017. Analysis on spatial-temporal features of taxis' emissions from big data informed travel patterns: a case of Shanghai, China. J. Cleaner Prod. 142, 926–935.
Martinez, L.M., et al., 2015. An agent-based simulation model to assess the impacts of introducing a shared-taxi system: an application to Lisbon (Portugal). J. Adv. Transp. 49, 475–495.
Newson, P., Krumm, J., 2009. Hidden Markov map matching through noise and sparseness. ACM, pp. 336–343.
Ntziachristos, L., et al., 2000. Copert iii. Computer Programme to calculate emissions from road transport, methodology and emission factors (version 2.1). European Energy Agency (EEA), Copenhagen.
Santi, P., et al., 2014a. Quantifying the benefits of vehicle pooling with shareability networks. Proc. Natl. Acad. Sci. 111, 13290–13294.
Santi, P., et al., 2014. Quantifying the benefits of vehicle pooling with shareability networks, 111, 13290-13294.
Santi, P., Ratti, C., 2017. A future of shared mobility. J. Urban Regen. Renew. 10, 328–333.
Shaheen, S., et al., 2016. Shared Mobility: Current Practices and Guiding Principles. U.S. Department of TransportaFon, Washington, D.C.
Shang, J., et al., 2014. Inferring gas consumption and pollution emission of vehicles throughout a city. ACM, pp. 1027–1036.
Spieser, K., et al., 2014. Toward a systematic approach to the design and evaluation of automated mobility-on-demand systems: A case study in Singapore. Springer, pp. 229–245.
Sun, D.J., Zhang, K., Shen, S., 2018. Analyzing spatiotemporal traffic line source emissions based on massive didi online car-hailing service data. Transp. Res. Part D: Transp. Environ. 62, 699–714.
Tachet, R., et al., 2017. Scaling Law of Urban Ride Sharing. Sci. Rep. 7, 42868.
Togawa, T., et al., 2016. Integrating GIS databases and ICT applications for the design of energy circulation systems. J. Cleaner Prod. 114, 224–232.
Vazifeh, M.M., et al., 2018. Addressing the minimum fleet problem in on-demand urban mobility. Nature 557, 534–538.
Xie, S., et al., 2006. Calculating vehicular emission factors with COPERTIII mode in China. Environmental. Science 3.
Xue, J.P., et al., 2010. Development of NOx emission inventory from motor vehicles in Hangzhou and study on its influence on air quality. Res. Environ. Sci. 23, 613–618.
Xue, M., et al., 2018. Possible emission reductions from ride-sourcing travel in a global megacity: the case of Beijing. J. Environ. Devel. 27, 156–185.
Yan, L., Wang, D., Zhang, S., Xie, D., 2019. Evaluating the multi-scale patterns of jobs-residence balance and commuting time–cost using cellular signaling data: a case study in Shanghai. Transportation 46, 777–792.
Yin, B., et al., 2018. Appraising the environmental benefits of ride-sharing: The Paris region case study. J. Cleaner Prod. 177, 888–898.
Yu, B., et al., 2017. Environmental benefits from ridesharing: A case of Beijing. Appl. Energy 191, 141–152.
Zachariah, J., et al., 2014. Uncongested mobility for all: A proposal for an area wide autonomous taxi system in New Jersey. Transportation Research Board 93rd Annual Meeting. Washington, DC.